Optimization of electrical properties of Cassiterite Nanoparticles by Iron Doping

***G Rubyshia Santhakumari, S John Kennady Vethanathan[1], K.U. Madhu[2]**
*Research Scholar, Department of Physics and Research Centre, St. Johns College, Palayamkottai
* (Affiliated to Manonmaniam Sundarnar University, Abishekapatti,Tirunelveli, Tamilnadu, India)
[1]Dept. of Physics, St. Johns College, Palayamkottai
[2]Dept. of Physics, S.T.Hindu College, Nagercoil
*e-mail: rubyshias@gmail.com

Abstract: Microwave assisted solution method was used to synthesize pristine and Iron (Fe) doped Cassiterite (SnO_2) nanoparticles. The effect of iron doping was characterized for the optimization of principal parameters of Cassiterite. The tetragonal structure of Cassisterite was confirmed through PXRD spectra. The particle size was calculated using Debye Scherrer formula and attains at nanometer range. The SEM image and EDX depicts the spherical structure and the composition of the elements of the synthesized nanoparticles. The optical band gap value is determined for the synthesized nanoparticle through the Tauc plot using Diffuse Reflectance Spectra. The specific capacitance value reveals the enhancement of electrical properties of Cassiterite through iron doping
Keywords: EDX, Nanoarticles, SEM, SnO_2, XRD

I. Introduction

The systems for energy storage with high energy storing capacity, low cost, and eco-friendly being necessary for the electronic gadgets Semiconductor metal oxides in nanometer size are considered in many researches as a consequence of their physical, chemical, magnetic and optical properties [3]. The present paper deals with post-transition metal oxide namely stannic oxide due to the optical transparency and wide optical band gap [8]. Iron (Fe) is one of the transition metal is used as the doping material due to ionic radius [9]. The aim of this paper is to enhance the principal parameters of SnO_2 by doping the iron through the characterization and focused on specific capacitance for the application of supercapacitor..

II. Synthesis method

The precursor of the nanoparticle synthesis was used as stannous chloride dihydrate ($SnCl_2{\cdot}2H_2O$), urea as catalyst and solvent as ethylene glycol. To enhance the principal parameters of Cassiterite, ferrous chloride ($FeCl_3$) was the doping material. The appropriate amounts of $SnCl_2.2H_2O$ and urea was added to ethylene glycol and heated at 540 W in a domestic microwave oven until the precipitate formation. Then washed with distilled water and acetone and the resultant was annealed at 400° C to get Cassiterite nanoparticles. As the addition of doping material at 8 wt%, iron doped Casseterite nanoparticles were synthesized.

III. Characterization Techniques

The synthesized nanoparticles XRD spectra were recorded by Powder X-ray Diffraction (PANalyticalX'PertPRO) with Cu Kα radiation (λ = 0.15406 nm) to reveal the structural parameters.The morphological analysis was carried out using SEM and the elemental composition analysis of the sample was done by EDX analysis (SEM-EDAX, JEOL 6390LA). The optical properties were analyzed by diffuse reflectance spectra (Agilent Cary 5000 UV-Vis spectrometer). Electrochemical characteristic studies were taken out using CH1604E Electrochemical workstation.

IV Results and Discussion

4.1 XRD analysis

Fig.1 shows the XRD spectra of pure and Fe doped SnO_2 nanoparticles. The intense and sharp peaks of spectra reveals the crystallinity nature and suited with JCPDS no 41-1445. The iron related reference peaks are not traced in the XRD spectra. The peaks of iron doped were wider and blue shift of 2θ than undoped Cassiterite. This results in particle size decrement [11].

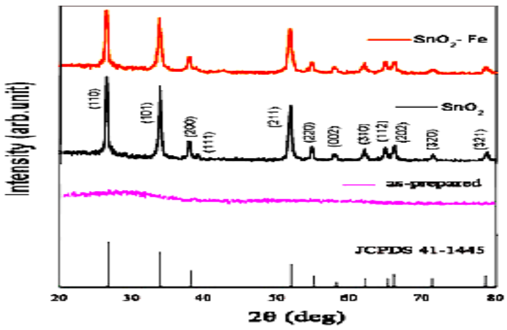

Fig. 1 XRD patterns of pristine and Fe doped Cassiterite nanoparticles

The Scherrer's formula was used to determine the particle size of the most intense XRD peak (110) were 27.49 and 10.25 nm of pristine and Fe doped Cassiterite[5]. The particle size was decrased after doping of Fe and confirms the incorporation of the iron ions into SnO_2 lattice successfully.

4.2. Morphological Analysis

Fig. 2a and Fig. 2b depicts the SEM images of pure and Fe doped SnO_2 nanoparticles. The spherical morphology are observed in the SEM image. EDX spectra Fig. 3a and Fig. 3b reveals the existence of Fe ions in the synthesized nanoparticle is confirmed through the Ni ions spectra.

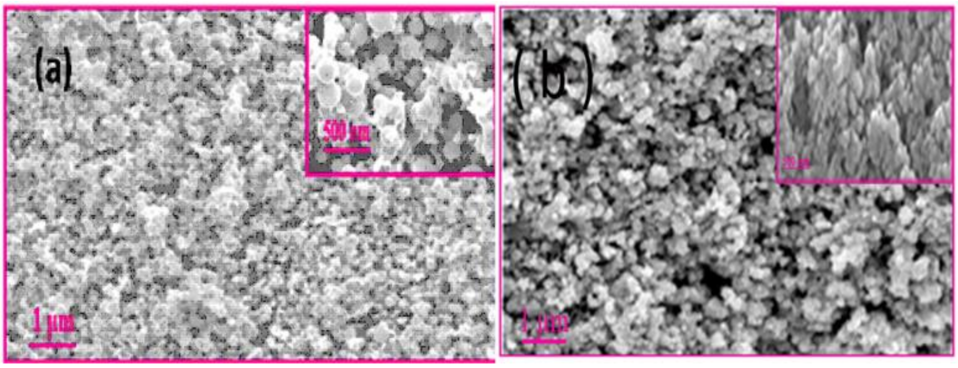

Fig. 2a and **Fig. 2b** SEM images SnO_2 and Fe doped SnO_2 nanoparticles

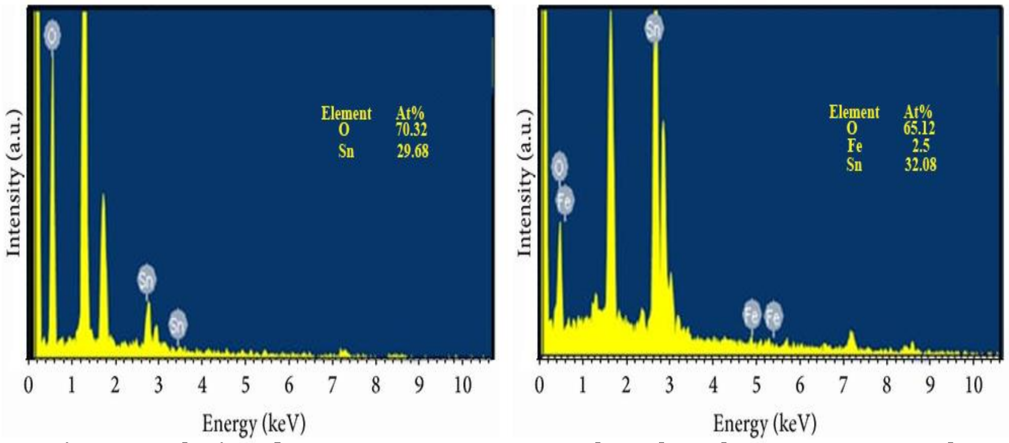

Fig. 3a and **Fig. 3b** EDX images SnO_2 and Fe doped SnO_2 nanoparticles

4.4. Band Gap Energy of Fe doped SnO_2 nanoparticles

The optical band gap energy E_g of the iron doped Cassiterite nanoparticles are calculated from the diffuse reflectance spectrum [10]. The E_g can be found out through the Tauc plot [11] is shown in the Fig. 4 and the extrapolation of linear region in the Tauc plot shows the value of 3.79 eV and 3.2 eV of stannic oxide and Fe doped stannic oxide nanoparticles

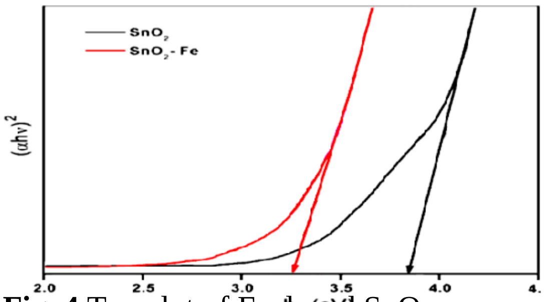

Fig. 4 Tau plot of Fe doped SnO_2 nano particles

4.4. Electrochemical studies

The pristine and Fe doped Cassiterite nanoparticles were examined using cyclic voltammetry (CV) and galvanostatic charge discharge (GCD) to study the electrochemical properties. Figure. 9 shows the CV curve for the scan rate 10-100 mV/s of pristine and Fe doped SnO_2 electrodes.

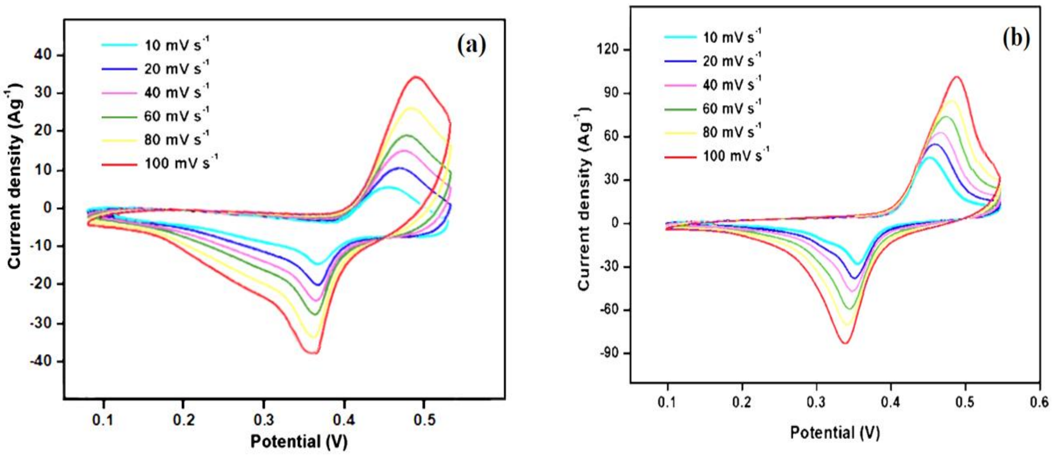

Fig. 5a and Fig. 5b CV curve of pristine and Fe doped Cassiterite nanoparticles

On increasing the scan rate, the position of redox peaks is shifted due to the reactions of faradaic [13]. The reduction of particle size of doped sample infers in the integrated surface area of electrodes. The GCD curve is shown in the Fig. 6a and Fig. 6b of pure and Fe doped SnO_2 electrodes at the current densities of 0.5–10 Ag^{-1}. The behavior of pseudocapacitance is clearly depicted through the GCD curve. The specific capacitance value were determined using from the GCD curve and Fe doped sample shows the highest value compared to the pristine Cassertite is shown in the plot of Fig. 7. Table 1shows the Specific capacitance of the prepared pure and Fe doped SnO_2 electrodes at diff erent current densities.

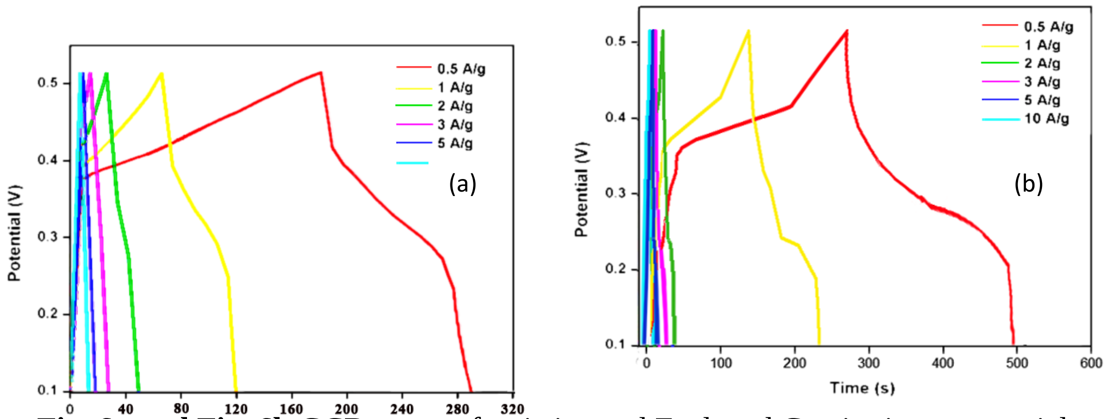

Fig. 6a and Fig. 6b GCD curve of pristine and Fe doped Cassiterite nanoparticles

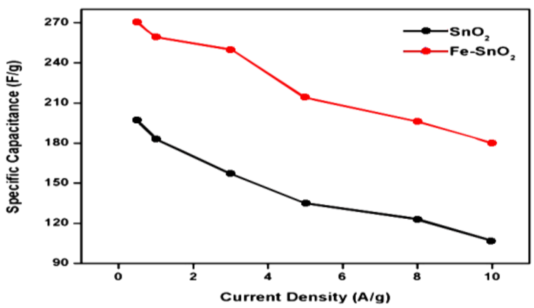

Fig. 7 Plot of current density(A/g) vs specific capacitance(F/g)

Table 1 Specific capacitance of pure and Fe doped SnO_2 electrodes

Current Density (A/g)	Specific capacitance (F/g)	
	SnO_2	Fe-SnO_2
0.5	198	272
1	184	258
2	159	251
3	136	216
5	121	197
10	108	181

V Conclusion

The Iron doped Cassiterite nanoparticles are synthesized successfully by microwave assisted solution method. The XRD pattern reveals that no other peaks related to iron oxides. The particle size decreases with iron doping. SEM shows that the particles are in spherical shape. From Tauc's plot, the optical band gap energy of the Fe doped SnO_2 nanoparticles are found. On increasing value of specific capacitance through iron doping on Cassiterite it can be suited for supercapacitor[14].

VI References

[1] Feng, Shu Fen Wang, Chun Feng Song, Meng Kai Lü, Yong Xin Qi, Guang Jun Zhou, Dong Xu, and Duo Rong Yuan 2003,'Synthesis and luminescence properties of SnO2 nanoparticles', Chemical Physics Letters, vol.3, no.4, pp.451-454.

[2] Ghobadi, Nader 2013,'Band gap determination using absorption spectrum fitting procedure', International Nano Letters, vol.3, no.1, pp. 1-4.

[3] Gu, F., Wang, S. F., Lü, M. K., Zhou, G. J., Xu, D., & Yuan, D.R. 2004, 'Photoluminescence properties of SnO2 nanoparticles synthesized by sol− gel method', The Journal of Physical Chemistry B, vol.108, no.24, pp. 8119-8123.

[4] Makuła, P., Pacia, M. and Macyk, W., 2018, 'How to correctly determine the band gap energy of modified semiconductor photocatalysts based on UV–Vis spectra', The journal of physical chemistry letters, vol. 9 no.23, pp.6814-6817.

[5] Patterson, A. L. 1939,'The Scherrer formula for X-ray particle size determination, Physical review, vol.56, no.10, pp. 978.

[6] Paulson, A., Sabeer, N.M. and Pradyumnan, P.P., 2018, 'Enhanced thermoelectric property of oxygen deficient nickel doped SnO2 for high temperature application', Materials Research Express, vol.5, no.4, pp.045511.

[7] Rani, S., Roy, S.C. and Bhatnagar, M.C., 2007,'Effect of Fe doping on the gas sensing properties of nano-crystalline SnO2 thin films', Sensors and Actuators B: Chemical, vol.122, no.1, pp.204-210.

[8] Salah, N., Habib, S., Azam, A., Ansari, M. S., & Al-Shawafi, W. M. 2016, 'Formation of Mn-doped SnO2 nanoparticles via the microwave technique: structural, optical and electrical properties', Nanomaterials and Nanotechnology, vol.6, pp. 17.

[9] Selamat, M. Z., Masron, F., Yusuf, M., Yusri, M., Kamarolzaman, A. A., Mohd Tahir, M., & Herawan, S. G. 2015. Effect of stannum on properties of graphite/stannum composite for bipolar plate', *In Applied Mechanics and Materials* vol.699, pp. 157- 162.

[10] Selvakumari, J. C., Ahila, M., Malligavathy, M., & Padiyan, D. P. 2017,'Structural, morphological, and optical properties of tin (IV) oxide nanoparticles synthesized using Camellia sinensis extract: a green approach', International Journal of Minerals, Metallurgy, and Materials, vol.24, no.9, pp. 1043-1051.

[11] Senthilkumar, V., Senthil, K. and Vickraman, P., 2012,'Microstructural, electrical and optical properties of indium tin oxide (ITO) nanoparticles synthesized by co-precipitation method', Materials Research Bulletin, vol.47, no.4, pp. 1051-1056.

[12] Suram, S. K., Newhouse, P. F., & Gregoire, J. M. 2016,'High throughput light absorber discovery, part 1: an algorithm for automated tauc analysis', ACS combinatorial science, vol.18 no.11, pp. 673- 681.

[13] Yang, Y., Ren, S., Ma, S., Hao, C. and Ji, M., 2015. Hollow tin dioxide microspheres with multilayered nanocrystalline shells for pseudocapacitor. Electrochimica Acta, vol.155, pp.437-446.

[14] Yang, Yang Jiao, Zhenglin Zhang, Fengyu Qu, Ahmad Umar, and Xiang Wu., 2014 "Hierarchical SnO2 nanostructures made of intermingled ultrathin nanosheets for environmental remediation, smart gas sensor, and supercapacitor applications." ACS applied materials & interfaces, vol.6, no. 3, pp. 2174-2184.

[15] R. B. Kadam, G. G Mali and B. S. Mohite, (2013). Analytical application of poly[dibenzo-18-crown-6] for chromatographic separation of thorium(IV) from uranium(VI) and other elements in glycine medium, *J. Radioanal. Nucl. Chem.295* (1) 501-511.

[16] R. B. Kadam, G. G Mali and B. S. Mohite, (2012). Development of analytical method for chromatographic separation of copper(II) using poly[dibenzo-18-crown-6]. *Int. J. Analytical and Bioanalytical Chemistry* ,2 (2) 139-146.

[17] K. R. Mahanwar, S. R. Sabale, R. B. Kadam and B. S. Mohite, (2012). Reversed-phase column extractive separation of Gd(III) with poly[dibenzo-18 crown-6],Int. *J. Inorganic Chemistry*, 2012.

[18] Kadam R. B. and Mohite B. S. (2014). Analytical application of poly[dibenzo-18- crown-6] for chromatographic separation of Cobalt(II) in glycine medium, *Res. J. Chem. Environ*.18 (3),7-18.

[19] R.Kadam, S. Jadhav, P. Kamble, N. Madane, (2022). Chromatographic Extraction of palladium(II) ions in multi-component mixture using poly[dibenzo-18-crown-6] as sorbent, *Journal of Emerging Technologies and Innovative Research*,9(4),141-154.

[20] N. S. Madane, R. B. Kadam, P. N. Kamble, (2022). Development of Reliable Analytical Method for Extraction and Separation of Zinc(II) in Kerosene, *The International journal of analytical and experimental modal analysis,* XIV (VII),1039-1042.

[21] R. Kadam, S. Jadhav., (2022). Reversed-Phase Column Extractive Separation of Palladium(II) with Poly[dibenzo- 18-crown-6]: A analysis of real sample,*Science, Technology and devolpement journal*, XI (VII),160-164.

[22] P.N. Kamble, N. S. Madane R.B. Kadam, (2023). Liquid-liquid extraction of Barium(II) using Cyanex 301 in Kerosene ,*The International journal of analytical and experimental modal analysis* ,XV (I),8-21.

[23] Pattnaik, S., Swain, K., Choudhury, P., Acharya, P.K., Mallick, S. (2009). Alfuzosin Hydrochloride Transdermal Films: Evaluation of Physicochemical, In Vitro Human Cadaver Skin Permeation and Thermodynamic Parameters. Int Brazil J Urol, 35(6): 716-729. doi: 10.1590/s1677-55382009000600010

[24] Mallick, S., Pattnaik, S., Swain, K., De, P. (2007). Interaction characteristics and thermodynamic behaviour of Gatifloxacin with aluminium hydroxide. Drug Dev Ind Pharm, 33(5):535-541. doi: 10.1080/03639040601050130

[25] Swain, K., Pattnaik, S., Mallick, S., Chowdary, K.A. (2009). Influence of hydroxypropyl methylcellulose on drug release pattern of a gastroretentive floating drug delivery system using a 32 full factorial design. Pharm Dev Technol, 14(2):193-198. doi: 10.1080/10837450802498902

[26] Swain, K., Pattnaik, S., Sahu, S.C., Mallick, S. (2009). Feasibility Assessment of Ondansetron Hydrochloride Transdermal Systems: Physicochemical Characterization and In vitro Permeation Studies. Lat Am J Pharm, 28(5): 706-714.

[27] Pattnaik, S., Swain, K., Mallick, S. (2009). Influence of Polymeric System and Loading Dose on Drug Release from Alfuzosin Hydrochloride Transdermal Films. Lat Am J Pharm, 28: 62-69.

[28] Pattnaik, S., Swain, K., Bindhani, A., Mallick, S. (2011). Influence of chemical permeation enhancers on Transdermal permeation of alfuzosin: An investigation using response surface modeling. Drug Dev Ind Pharm, 37(4): 465-474. doi: 10.3109/03639045.2010.522192

[29] Pattnaik, S., Pathak, K. (2017). Mesoporous Silica Molecular Sieve Based Nanocarriers: Transpiring Drug Dissolution Research. Curr Pharm Des, 23(3): 467-480. doi: 10.2174/1381612822666161026162005

[30] Pattnaik, S., Swain, K., Rao, J.V., Talla, V., Prusty, K.B., Subudhi, S.K. (2015). Polymer co-processing of ibuprofen through compaction for improved oral absorption. RSC Adv, 5 (91), 74720-74725. https://doi.org/10.1039/C5RA13038G

[31] Pattnaik, S., Swain, K., Manaswini, P., Divyavani, E., Rao, J.V., Talla, V., Subudhi, S.K. (2015). Fabrication of aceclofenac nanocrystals for improved dissolution: Process optimization and physicochemical characterization. J Drug Deliv Sci Technol, 29:199-209. https://doi.org/10.1016/j.jddst.2015.07.021

[32] Pattnaik, S., Swain, K., Rao, J.V., Talla, V., Subudhi, S.K. (2015). Aceclofenac nanocrystals for improved dissolution: influence of polymeric stabilizers. RSC Adv, 5 (112), 91960-91965. https://doi.org/10.1039/C5RA20411A

[33] Mahapatra, A.K., Murthy, P.N., Patra, R.K., Pattnaik, S. (2013). Solubility Enhancement of Modafinil by Complexation with β-cyclodextrin and hydroxypropyl β-cyclodextrin: A Response Surface Modeling Approach. Drug Delivery Letters, 3(3): 210-219. doi:10.2174/22103031113039990005

[34] Swain, K., Pattnaik, S., Yeasmin, N., Mallick, S. (2011). Preclinical evaluation of drug in adhesive type ondansetron loaded transdermal therapeutic systems. Eur J Drug Metab Pharmacokinet, 36 (4), 237-241. doi: 10.1007/s13318-011-0053-x

[35] Pattnaik, S., Swain, K., Rao, J.V., Talla, V., Mallick, S. (2015). Temperature influencing permeation pattern of alfuzosin: An investigation using DoE. Medicina, 51(4):253-261. doi: 10.1016/j.medici.2015.07.002

[36] Hota, S.S., Pattnaik, S., Mallick, S. (2020). Formulation and Evaluation of Multidose Propofol Nanoemulsion Using Statistically Designed Experiments. Acta Chimica Slovenica, 67(1): 179-188.

[37] Panda, D.S., Alruwaili, N.K., Pattnaik, S., Swain, K. (2022). Ibuprofen loaded electrospun polymeric nanofibers: A strategy to improve oral absorption. Acta Chimica Slovenica, 69(2), 483–488. doi: 10.17344/acsi.2022.7370

[38] Vijayalakshmi A, Vidyavathy Balraj (2017), 'Optical, thermal, laser damage threshold, dielectric studies and z-scan technique of novel semiorganic NLO material: sodium boro succinate (NaBS)', U.P.B. Scientific Bulletin- Series B, vol. 79, issue 1, pp. 221-232.

[39] Vijayalakshmi A, Vidyavathy Balraj, Determination of basic solid state parameters and characterization of optical, dielectric and fluorescence properties of Calcium Boro Lactate(CaBL) , Journal of chemical society, Pakistan. Vol. 38 Issue 6, pp. 1092-1097.

[40] Vijayalakshmi A, Vidyavathy Balraj, G. Vinitha, (2016),"Crystal structure, growth and nonlinear optical studies of Isonicotinamide p-nitrophenol: A new organic crystal for optical limiting applications", Journal of crystal growth, 448 pp.82-88.
doi: https://doi.org/10.1016/j.jcrysgro.2016.05.002

[41] Vijayalakshmi A, Vidyavathy Balraj , Vinitha G. , (2016) "Structure and characterization of a new organic crystal for optical limiting applications, isonicotinamide bis-p-aminobenzoic acid", Ukranian J. Phys. Opt., Volume 17, Issue 3.pp. 98-104.

[42] Vijayalakshmi A, Vidyavathy, B, Peramaiyan, G & Vinitha, G (2017), 'Synthesis, growth, structural and optical studies of a new organic three dimensional framework: 4-(aminocarbonyl) pyridine 4 (aminocarbonyl) pyridinium hydrogen L-malate, Journal of Solid State Chemistry, vol. 246, pp. 237-244. doi: https://doi.org/10.1016/j.jssc.2016.11.025

[43] Vijayalakshmi A, Vidyavathy Balraj , B. Gunasekaran, Abdul Razack Ibrahim, Synthesis, Structural, Optical, Thermal and LDT Characterization of Novel Semi-Organic Non-Linear Optical Material: Calcium Borolactate, Asian Journal of Chemistry; Vol. 28, No. 12 (2016).

[44] Padmaja, D. L., Nagaprasad, S., Pant, K., & Kumar, Y. P. (2022). Role of Artificial Intelligence and Deep Learning in Easier Skin Cancer Detection through Antioxidants Present in Food. *Journal of Food Quality*, *2022*.

[45] Padmaja, D. L. (2021). Performance Analysis of Different Architectures on Face Mask Detection. *Turkish Journal of Computer and Mathematics Education (TURCOMAT)*, *12*(13), 377-381.
[46] Gundu, K. S., Dhyaram, L. P., Ramana Rao, G. N. V., & Surya Deepak, G. (2023, January). Comparative Analysis of Energy Consumption in Text Processing Models. In *Advancements in Smart Computing and Information Security: First International Conference, ASCIS 2022, Rajkot, India, November 24–26, 2022, Revised Selected Papers, Part I* (pp. 107-116). Cham: Springer Nature Switzerland.
[47] Ramirez-Asis, E., Guzman-Avalos, M., Mazumdar, B. D., Padmaja, D. L., Mishra, M., Hirolikar, D. S., & Kaliyaperumal, K. (2022). Metaheuristic Methods for Efficiently Predicting and Classifying Real Life Heart Disease Data Using Machine Learning. *Mathematical Problems in Engineering*, *2022*.
[48] Padmaja, D. L., Tammali, S., Gajavelly, N., & Reddy, K. S. (2022, May). A comparative study on natural disasters. In *2022 International Conference on Applied Artificial Intelligence and Computing (ICAAIC)* (pp. 1704-1709). IEEE.
[49] Padmaja, D. L., Sruthi, B. S., Deepak, G. S., & Harsha, G. S. (2022, April). Analysis to Predict Coronary Thrombosis Using Machine Learning Techniques. In *2022 International Conference on Sustainable Computing and Data Communication Systems (ICSCDS)* (pp. 21-27). IEEE.
[50] Padmaja, D. L., & Sriharsha, G. K. (2022, December). Challenges in Crop Selection Using Machine Learning. In *Artificial Intelligence and Data Science: First International Conference, ICAIDS 2021, Hyderabad, India, December 17–18, 2021, Revised Selected Papers* (pp. 66-76). Cham: Springer Nature Switzerland.
[51] Padmaja, D. L., Nagaprasad, S., Pant, K., & Kumar, Y. P. (2022). Role of Artificial Intelligence and Deep Learning in Easier Skin Cancer Detection through Antioxidants Present in Food. *Journal of Food Quality*, *2022*.
[52] Baker, M. R., Padmaja, D. L., Puviarasi, R., Mann, S., Panduro-Ramirez, J., Tiwari, M., & Samori, I. A. (2022). Implementing Critical Machine Learning (ML) Approaches for Generating Robust Discriminative Neuroimaging Representations Using Structural Equation Model (SEM). *Computational and Mathematical Methods in Medicine*, *2022*.
[53] Lakshmipadmaja, D., & Vishnuvardhan, B. (2018). Classification performance improvement using random subset feature selection algorithm for data mining. *Big Data Research*, *12*, 1-12.
[54] Padmaja, D. L., & Vishnuvardhan, B. (2018). Evaluating the influence of parameter values on the performance of random subset feature selection algorithm on scientific data. *Data & Knowledge Engineering*, *117*, 174-182.
[55] Padmaja, D. L., & Vishnuvardhan, B. (2016, February). Comparative study of feature subset selection methods for dimensionality reduction on scientific data. In *2016 IEEE 6th International Conference on Advanced Computing (IACC)* (pp. 31-34). IEEE.
[56] Dhyaram, L. P., & Vishnuvardhan, B. (2018). RANDOM SUBSET FEATURE SELECTION FOR CLASSIFICATION. *International Journal of Advanced Research in Computer Science*, *9*(2).
[57] Padmaja, D. L., & Vishnuvardhan, B. (2014). Survey of dimensionality reduction and mining techniques on scientific data. *International Journal of Computer Science & Engineering Technology*, *1*(5), 1062-6.
[58] Padmaja, D. L., & Vishnuvardhan, B. INFLUENCE OF DATA GEOMETRY IN RANDOM SUBSET FEATURE SELECTION.
[59] Lakshmi Padmaja, D., & Vishnuvardhan, B. (2019). Variance-based feature selection for enhanced classification performance. In *Information Systems Design and Intelligent Applications: Proceedings of Fifth International Conference INDIA 2018 Volume 1* (pp. 543-550). Springer Singapore.
[60] Padmaja, D. L., Surya Deepak, G., Sriharsha, G. K., & Ramana Rao, G. N. V. (2021). Ensemble Methods for Scientific Data—A Comparative Study. In *Information and*

Communication Technology for Competitive Strategies (ICTCS 2020) Intelligent Strategies for ICT (pp. 587-595). Singapore: Springer Nature Singapore.

[61] Nagaprasad, S., Padmaja, D. L., Qureshi, Y., Bangare, S. L., Mishra, M., & Mazumdar, B. D. (2021). Investigating the impact of machine learning in pharmaceutical industry. *J. Pharm. Res. Int.*, *33*, 6-14.

[62] Sriharsha, G. K., Padmaja, D. L., Rao, G. R., & Deepa, G. S. (2022, December). A Modified Approach of Hyper-parameter Optimization to Assess The Classifier Performance. In *2022 IEEE Pune Section International Conference (PuneCon)* (pp. 1-9). IEEE.